BACK-SURFACE PASSIVATION FROM THE APPLICATION OF INEXPENSIVE SPRAY/SPIN ON POLYMER COATINGS

Authors: Andrew Thomson[+], Teng Kho[+], Paul Williams[*], Ari Karkkainen[*], Thomas Allen[+] and Andres Cuevas[+]

[+]Research School of Engineering, Australian National University, Canberra ACT 0200, Australia
[*]Optitune International Pte. Ltd., www.optitune.com

ABSTRACT: Inexpensive spray/spin-on polymer dielectric films are investigated for their suitability to passivate the rear-surface of c-Si solar cells. A number of different Optitune polymer compositions were trialled. So far the best material achieves SRV of 110 cm/s when applied to 0.8 Ω·cm p-type silicon and 64 cm/s on 5 Ω·cm n-type. Similar films show passivation on boron diffusions which are stable after annealing at 700 °C, and do not suffer degradation when submitted to standard humidity degradation tests for 10,000 hours. We believe the passivation demonstrated and benefits regarding improved back-surface reflections (discussed in 2CV.5.54, in this conference), make these dielectric films an attractive option for improving existing fabrication lines. This is particularly true given the cost benefits of spray techniques compared to PECVD or ALD technologies.

Keywords: Passivation, Silicon, Rear surface

1. INTRODUCTION

Many approaches are being trialled to further improve the performance and cost-effectiveness of c-Si solar cells. Most full under the following categories:

- Selective emitter formation, and front surface passivation [1].
- Dielectric back-surface passivation, with non-diffused or diffused point contacts [2].
- Conversion to n-type silicon, a material more tolerant to metallic impurities [3].
- Rearrangement of device architecture, such as the fabrication of rear contact devices [4].
- Alternative junction formation either by, ion-implantation, or hetero-junction formation [4, 5].

In general, these aforementioned solutions require considerable capital expenditure to be included in existing fabrication lines. The most likely exception, perhaps, is the some of the more ingenious selective emitter formation techniques see ref [6] for an example.

Back-surface passivation is also strongly considered as a cost-effective option for improving industrial solar cells [7]. Many publications regarding Al_2O_3 demonstrate its ability to passivate in combination with dielectric stacks and a number of fabrication procedures have been developed. Further, deposition technologies have progressed such that it can be deposited at speed on an industrial scale [8].

However current Al_2O_3 based techniques require the ability to coat with an additional two dielectric films (a thin Al_2O_3 and thicker capping layer). Furthermore these techniques generally require toxic precursors, vacuums and plasmas. These factors are often costly in large scale production. We investigate the solution of spin/spray on films that passivate and do not require a capping layer. Additionally, in a related paper submitted to these proceedings we show these films perform excellently as a back reflectors [9].

The polymer wet-chemicals used to produce the passivating films investigated here are synthesised by Optitune, Finland. There is the possibility to apply these films via industrial techniques such as ultrasonic spray coating, APCVD, roller coating and ink-jet printing.

We outline our fabrication and characterisation techniques used to quantify different films' passivating abilities. In the results section, we present photoconductance measurements of recombination demonstrating the effect of the films. Finally the results are discussed.

2. METHODOLOGY

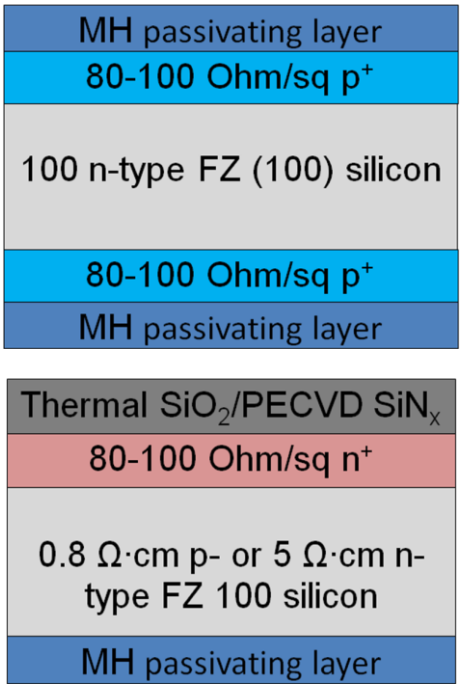

Figure 1: diagram photoconductance test-structures used to study the passivating effects of Optitune films. The top symmetrical structures are boron diffused double sided and the bottom asymmetrical samples are phosphorus diffused, and represent a pseudo solar cell.

Symmetrical Boron Diffused Sample

In order to fabricate symmetrical boron diffused samples 100 Ω cm n-type 4" (100) FZ wafers were acid etched to remove saw damage, and subsequently RCA cleaned. Post cleaning, the wafers received a BBr_3 diffusion in a Tempress Quartz furnace at 860 °C, with and oxygen cool down, resulting in 100 Ω/sq diffusions.

The wafers were then deglazed in HF, and were found to be hydrophobic indicating successful removal of the boron glass. The wafers were then coated on both surfaces with the Optitune MH coatings, as described in the following section, and annealed. At each processing stage the J_{0e} was monitored with a WCT-120.

Asymmetrical phosphorus diffused samples

Wafers used in this study were 4" Fz, (100), 0.8 Ω cm p-type or 5 Ω cm n-type, to observe the effect of wafer doping. Further, the n-type wafers' doping enabled high-injection τ_{eff} measurements and therefore determination of the single sided emitter-saturation current density J_{0e} [10]. All wafers were saw-damaged etched in HF/HNO_3 removing a minimum 10 µm of silicon from both surfaces. Prior to diffusion and oxidation steps the samples were given a standard RCA clean to prevent contamination.

Single-sided $POCl_3$ phosphorus diffusions 100 Ω/sq were formed. Either by photoresist-masked etch back in TMAH of double side diffused wafers or single-side thermal-SiO_2 masking prior to diffusion.

After single-side diffusion formation all wafers were given a high-quality thermal oxidation, to afford effective emitter passivation. Whereupon the SiO_2 on the non-diffused surface was removed by HF fuming.

Optitune polymer films were spin coated and baked at 200 °C for 5 mins see accompanying paper [9] for more details. Table 1, idetifies the material label. Annealing was performed in a temperature controlled quartz funrace, under a nitrogen ambient. Figure 1 depicts the sample sturctres that resulted from the aformentioned processes.

Measurements of back surface recombination

To measure the back-surface recombination, first the J_{0e} of the front emitter was determined from the n-type wafers. Second, the total recombination was measured for samples passivated by Optitune films before and after different series of annealing. In this case the effective recombination rate is given by

$$R_{\text{eff}} = \frac{\Delta n}{\tau_{\text{eff}}} = \frac{\Delta n}{\tau_{\text{bulk}}} + \frac{S_{\text{eff,back}}\Delta n}{W} + \frac{J_{0e}\Delta n(\Delta n + N_{\text{Dop}})}{W n_i^2 q}$$

Hence when τ_{eff} and J_{0e} are known, a combined recombination representing the effective bulk and rear-surface recombination can be determined.

To determine a measure of back surface SRV we used

$$S_{\text{eff,back, UL}} = \frac{W}{\tau_{\text{eff}}(\Delta n)} - \frac{J_{0e}(\Delta n + N_{\text{Dop}})}{n_i^2 q}$$

Where $S_{\text{eff,back, UL}}$ is the upper limit on back surface effective SRV owing to the assumption that bulk recombination is minimal. This is reasonable as the starting material is FZ, and the phosphorus diffusion protects the wafer bulk from further contamination during annealing.

3. RESULTS

Symmetrical boron-diffused surface passivation

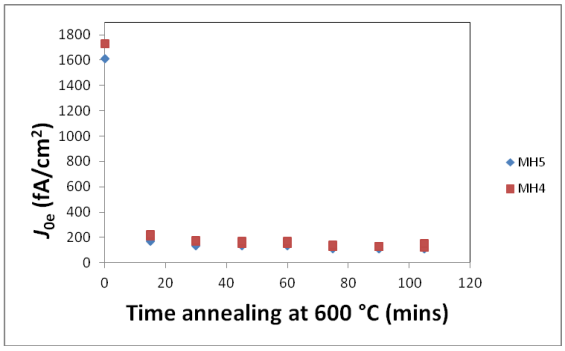

Figure 2: Boron diffused surface J_{0e} plotted as a function of annealing time at 600 °C, in N_2 in a quartz furnace.

Figure 2 plots the J_{0e} of boron-diffused samples as a function of annealing time at 600 °C, where time zero represents the as bake passivation. Similar levels of passivation are achieved by both of the MH materials. Initially after baking the passivation drops from 1800 to 200 fA/cm^2. With extended annealing time the J_{0e} further drops to 100 fA/cm^2. While not directly relevant to rear-surface passivation this experiment demonstrates suitable annealing conditions to improve the passivation.

Asymmetrical rear surface passivation

As our lifetime structures are asymmetrical they are not straight forward to analyse, hence we make a number of plots in order to explain the results in Table 1 which globally summarises our $S_{\text{eff,back,ul}}$ results. Firstly, we give an example of measurements on 5 Ω·cm n-type silicon, as the doping (1×10^{15} cm^{-3}) is such that high-injection measurements can be made and the single-side J_{0e} can de directly determined, from the slope of the inverse τ_{eff}. Figure 3 a) plots the inverse lifetime of a sample coated with MH6 (Al_2O_3).

We find that with annealing time at 500 °C recombination decreases. Further that the J_{0e}—represented by the linear fit to the high-injection data in Figure 2 a)—is fairly constant. Hence changes in recombination are caused by a reduction in the rear SRV.

To demonstrate how inverse recombination can be viewed additively, we have modelled a recombination curve for a sample with no rear-surface or bulk recombination and a J_{0e} of 172 fA/cm^2 and plotted this in Figure 3 a). The subtraction of the inverse-emitter recombination from the inverse τ_{eff} gives the combined bulk and back-surface recombination, $S_{\text{eff,back,ul}}$, plotted in Figure 3 b). We find that as the anneal time increases the $S_{\text{eff,back,ul}}$ is decreasing. In this case we find the trend of $S_{\text{eff,back,ul}}$ with Δn is consistent with SRH recombination with a Δn transitioning from high to low injection.

The effectiveness of Optitune material passivation on more heavily doped silicon—in this case 0.8 Ω·cm p-type silicon where $N_a=2\times10^{16}$ /cm^3—was also measured. The effectiveness of MH4 passivation is demonstrated in Figure 4 where the sample was annealed at 600 °C.

Figure 4 a) plots the τ_{eff} as a function of Δn. Also included is the τ_{eff} limit imposed by the front surface. We find that with increasing anneal time the rear SRV is reduce to the point where it is small compared to the front surface recombination. This is better illustrated in Figure 4 b) which plots the inverse τ_{eff}. The $S_{eff,back,ul}$ is also given in Figure 4 c). Also included in Figure 4 c), is an axis that gives an equivalent scaling of surface recombination equated to low injection emitter recombination. This scale in fA/cm^2 allows for comparison with measurements of rear diffused emitters.

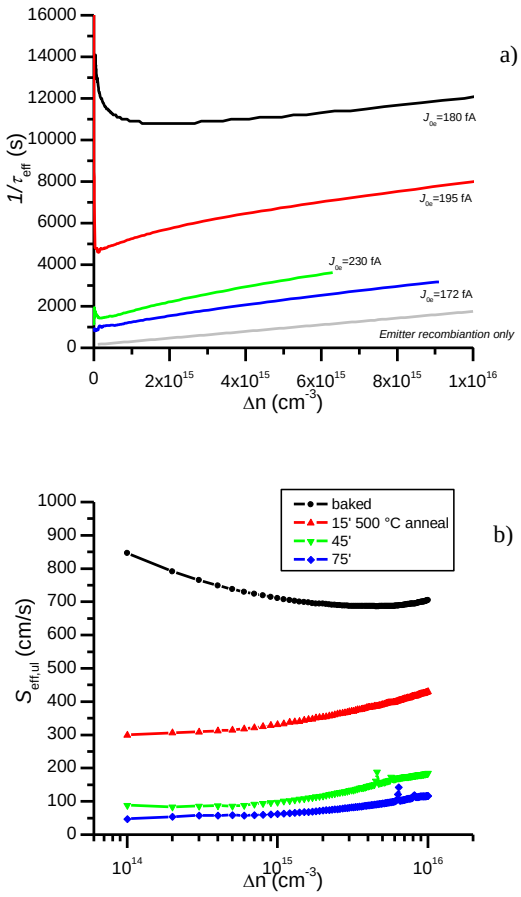

Figure 3: measurements of recombination for samples fabricated with 5 Ω·cm n-type wafers, measured after annealing at 500 °C for different intervals. Plot a) Inverse-effective lifetime plotted versus Δn. Plot b) the upper limit of SRV for the rear surface calculated by removing the front-surface emitter recombination, plotted as a function of Δn.

The same analysis described by Figure 3 and Figure 4 was applied to identically structured samples, but with different back-surface coatings. For each case, the back surface recombination was determined after annealing, and is summarised at a single injection level in Table 1. The injection level used was $\Delta n = 2\times10^{14}$ (p-type) and $\Delta n = 2\times10^{15}$ (n-type), which is the approximate 1 sun operation point given the doping if the passivation is reasonable. We see that MH6 effectively passivates the n-type surface, and reasonable passivation is achieve in the p-type surfaces for the MH4 and MH5 materials.

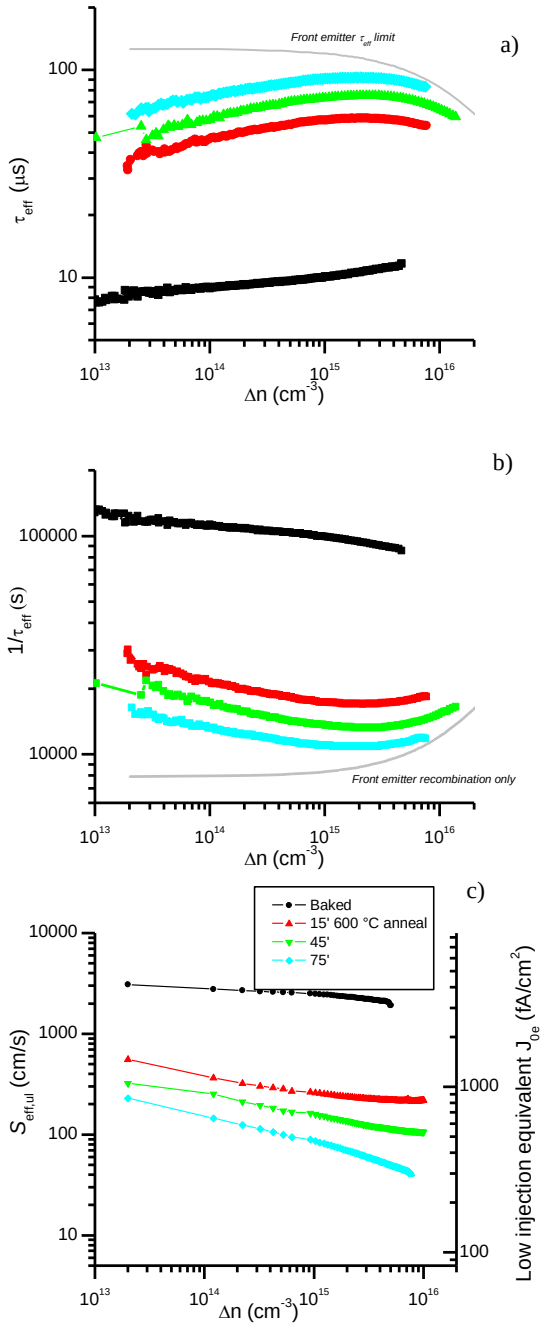

Figure 4: measurements of recombination for samples fabricated with 0.8 Ω·cm p-type wafers, measured after annealing at 600 °C for different intervals. Plot a) τ_{eff} versus Δn depicting the upper-limit imposed by the front-surface emitter. Plot b) inverse-effective lifetime plotted versus Δn. Plot c) the upper limit of SRV for the rear surface calculated by removing the front-surface emitter recombination, plotted as a function of Δn.

Table 1: $S_{eff,back,UL}$ measured for different materials after similar annealing experiments presented in Figures 2 and 3. $S_{eff,back,UL}$ was taken at Δn relevant to the wafers' 1 sun point of operation.

Material	Anneal	SRV 0.8 ohm p-type (cm/s)	SRV 5 Ω-cm n-type (cm/s)
MH1	500/600 N_2	1200	284
MH4	500/600 N_2	110	205
MH5	600 N_2	150	
MH6	500 N_2	465	64

Simplified processing

1 Ω cm p-type were prepared as described above for the single-sided phosphorus diffusion. However the thermal SiO_2 was replaced with a stoichiometeric PECVD SiN_x grown in a Roth and Rau AK400, passivating the front n^+ diffused surface.

For these samples the front surface J_{0e} was determined from separate measurements of symmetrical 100 Ω-cm n-type with identical surface diffusions and SiN_x passivation.

Similarly to the results in the previous section the passivation of samples with different rear coatings were measured after annealing at 600 °C for 15 mins in N_2 and subsequently a 400 °C 30 mins anneal in forming gas. Reasonable rear passivation is achieved as evidenced in Figure 5. We find in this case reasonable rear surface passivation is achieved with the MH4 and MH5 materials.

4. DISCUSSION

From our results, changes in recombination resulting from improvements in back surface passivation were measured. These structures are essentially pseudo cells, where the level of passivation afforded is relevant (<500 cm/s) is considerably better than that typically achieved by Al BSF [7], on silicon that quite highly doped (=2×10^{16} /cm^3). Additionally the industrial application of these materials could have considerable cost benefits compared to state-of-the-art back surface passivation techniques. Finally, reasonable passivation was achieved with different material compositions, indication these films can be designed for different process requirements.

Future studies will include the fabrication of rear passivated solar cells, compared to an Al BSF reference.

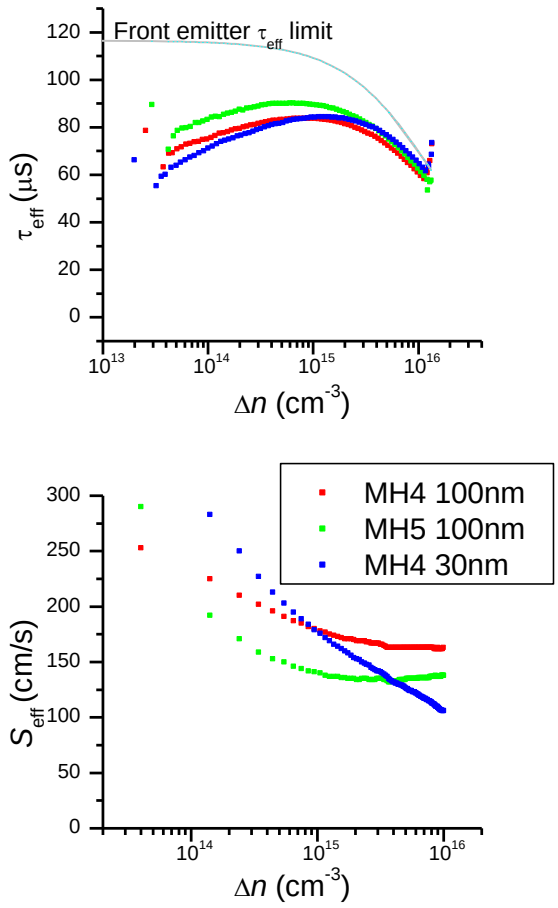

Figure 5: τ_{eff} and $S_{eff,UL}$ plotted as a function of Δ*n* for samples with different rear MH coatings. Samples fabricated with front SiN_x passivation on phosphorus diffusions.

REFERENCE:

1. Hanh, G. *Status of selective emitter technology*. in *European Photovoltaic Solar Energy Conference*. 2010. Valencia, Spain.
2. Lauermann, T., et al. *Enabling dielectric rear side passivation for industrial mass production by developing lean printing-based solar cell processes*. in *Photovoltaic Specialists Conference (PVSC), 2010 35th IEEE*.
3. Osborne, M., *Trina Solar to develop n-type silicon solar cells with Australian National University*, in http://www.pv-tech.org/news/trina_solar_to_develop_n_type_silicon_solar_cells_with_australian_national. 2011.
4. Meijun, L., et al., *Interdigitated back contact silicon heterojunction solar cell and the effect of front surface passivation.* Applied Physics Letters, 2007. **91**(6): p. 063507.
5. Meier, D.L., et al., *N-Type, Ion-Implanted Silicon Solar Cells and Modules.* Photovoltaics, IEEE Journal of, 2011. **1**(2): p. 123-129.
6. Antoniadis, H., et al. *All screen printed mass produced Silicon Ink selective emitter solar cells*. in *Photovoltaic Specialists Conference (PVSC), 2010 35th IEEE*.
7. Altermatt, P.P., et al., *HIGLY PREDICTIVE MODELLING OF ENTIRE $\mathrmSi$ SOLAR CELLS FOR INDUSTRIAL APPLICATIONS.* Proceedings of the

24th European Photovoltaic and Solar Energy Conversion, Hamburg, Germany, 2009.
8. Werner, F., et al., *High-rate atomic layer deposition of Al2O3 for the surface passivation of Si solar cells.* Energy Procedia. **8**(0): p. 301-306.
9. Thomson, A., T. Kho, and A. Cuevas. *Enhanced back-surface reflectance from the application of inexpensive spray/spin on polymer coatings*. in *This conference*. 2012.
10. Kane, D.E. and R.M. Swanson, *Measurement of the emitter saturation current by a contactless photoconductivity decay method.* Proceedings of the 18th IEEE Photovoltaic Specialists Conference, Las Vagas, USA., 1985.